Performance of a Light-Weight Ablative Thermal Protection Material For the Stardust Mission Sample Return Capsule

M. A. Covington

ELORET Corporation, 690 W. Fremont Ave., Suite 8, Sunnyvale CA 94087
acovington@mail.arc.nasa.gov

ABSTRACT

New tests and analyses are reported that were carried out to resolve testing uncertainties in the original development and qualification of a lightweight ablative material used for the Stardust spacecraft forebody heat shield. These additional arcjet tests and analyses confirmed the ablative and thermal performance of low density Phenolic Impregnated Carbon Ablator (PICA) material used for the Stardust design. Testing was done under conditions that simulate the peak convective heating conditions (1200 W/cm^2 and 0.5 atm) expected during Earth entry of the Stardust Sample Return Capsule. Test data and predictions from an ablative material response computer code for the in-depth temperatures were compared to guide iterative adjustment of material thermophysical properties used in the code so that the measured and predicted temperatures agreed. The PICA recession rates and maximum internal temperatures were satisfactorily predicted by the computer code with the revised properties. Predicted recession rates were also in acceptable agreement with measured rates for heating conditions 37% greater than the nominal peak heating rate of 1200 W/cm^2. The measured in-depth temperature response data show consistent temperature rise deviations that may be caused by an undocumented endothermic process within the PICA material that is not accurately modeled by the computer code. Predictions of the Stardust heat shield performance based on the present evaluation provide evidence that the maximum adhesive bondline temperature will be much lower than the maximum allowable of 250˚C and an earlier design prediction. The re–evaluation also suggests that even with a 25 percent increase in peak heating rates, the total recession of the heat shield would be a small fraction of the as-designed thickness. These results give confidence in the Stardust heat shield design and confirm the potential of PICA material for use in new planetary probe and sample return applications.

1. INTRODUCTION

The renewed interest in space missions to explore other planets has created a need for new advanced heat shield materials capable of efficiently protecting spacecraft under very high heating conditions. Such conditions may be experienced both during entry into the atmospheres of planets of interest and during reeentry into Earth's atmosphere for return missions. Very little development of new, efficient ablative materials has been pursued in the past two decades (since the Apollo and Viking spacecraft) due partly to the lack of missions requiring such materials.

The Stardust mission, as part of NASA's Discovery Program in 1995, created a requirement for new ablative heat shields as an enabling technology to meet the spacecraft mass goals. The Stardust mission [1] was designed as a mission to fly by the comet, Wild 2, at close range for the collection of cometary debris as well as to obtain interplanetary dust samples and return them to Earth within a Sample Return Capsule (SRC). The success of the mission requires that this Sample Return Capsule protect the collected samples during Earth atmospheric entry at an inertial velocity of 12.6 km/sec by keeping the SRC internal structure at temperatures that meet a science requirement to keep the sample materials below 70°C. These conditions result in nominal values for stagnation point heating flux of 1200 W/cm^2, peak surface pressures of 0.5 atm, and an integrated heat load of 36.5 kJ/cm^2 for the baseline entry.

To meet the requirements for the Stardust mission, one of a family of lightweight ceramic ablator materials developed at NASA Ames Research Center was selected for the forebody heat shield of the Stardust Sample Return Capsule. This material, Phenolic Impregnated Carbon Ablator (PICA), consists of a commercially available low density carbon fiber matrix substrate impregnated with phenolic resin. Some char-

acteristics of this family of lightweight ablator materials and processing methods are given in [2]. The Stardust program resulted in intensive material development, modeling, and testing efforts [3] to provide a heat shield for the high convective heating conditions expected during Earth entry while under constraints of limited time and funding. Because of uncertainties in the heating rate calibrations carried out under the original test activities, a second project was initiated to reexamine the arcjet test conditions, the PICA ablative and thermal performance, and the modeling used to design the Stardust flight heat shield. Details of this project are reported in [4], and the summarized results are presented in this paper.

2. TESTS AND ANALYSES

2.1 PICA Material Description

The material used for the Stardust forebody heat shield is one of a class of low density, charring ablative materials recently developed at the NASA Ames Research Center. The PICA material is made from a fibrous carbon matrix insulation (Fiber Materials, Inc. under the trade name Fiberform®) impregnated with a commercial phenolic resin. The phenolic-formaldehyde resin (Borden Chemical SC1008®) used in the Starudust formulation creates a porous thermoset material after polymerization that has final bulk densities ranging from 0.22 to 0.27 g/cm^3, depending on the processing employed. More extensive details of the processing of PICA materials are given in [2].

2.2 Arc Jet Tests

The tests and related analyses were carried out to investigate the performance of PICA under conditions appropriate to the Stardust SRC entry environment. The test program utilized tests in a high energy arc jet to obtain needed data on both the ablative performance and the thermal performance of PICA material by varying the model size and the arc jet operating conditions.

The NASA Ames 60 MW Interaction Heating Facility [5] was used to provide the aerothermal test environment required to simulate Stardust SRC entry conditions as it was for the earlier Stardust development and qualification testing. Sixteen PICA flat-faced cylindrical models of 2.54 cm and 5.08 cm diameters were tested to obtain ablative performance data at the approximate conditions expected at the SRC peak convective heating flux and for heating rates at a required heat shield design margin above this. To measure thermal performance, sixteen flat-faced cylindrical models of 10.16 cm diameter were tested at lower convective heating rate conditions. Radiation heating from the entry shock layer previously had been found to be unimportant for the Stardust mission [6] as was the case for these arc jet tests. A summary of the configurations of these models and their test conditions are given in Tables 1 and 2. The stream enthalpy values in Tables 1 and 2 were deduced from laminar flow heat transfer relationships [7] using the measured pitot pressure and stagnation point heat flux to both copper heat sink calorimeters and water-cooled calorimeters.

Table 1. 2.54 cm and 5.08 cm diameter PICA models and test conditions

Model No.	Run No.	Model Diameter (cm)	Test Time (sec)	Heating Rate (W/cm^2)	Heat Load (kJ/cm^2)	Stagnation Pressure (atm)	Enthalpy (MJ/kg)	PICA Thickness (cm)	PICA Thickness (inch)
23	12E	2.54	15	1630	24.5	0.65	29.5	5.72	2.252
22	12W	2.54	10	1630	16.3	0.65	29.5	5.72	2.252
26	14E	2.54	20	1630	32.6	0.65	29.5	5.72	2.252
24	14W	2.54	10	1630	16.3	0.65	29.5	5.72	2.252
28	15E	2.54	15	1630	24.5	0.65	29.5	5.72	2.252
27	15W	2.54	6	1630	9.8	0.65	29.5	5.72	2.252
30	16E	2.54	22	1630	35.9	0.65	29.5	5.72	2.252
29	16W	2.54	17	1630	27.7	0.65	29.5	5.72	2.252
10	9E	5.08	30	1150	34.5	0.65	29.5	5.66	2.228
11	9W	5.08	20	1150	23.0	0.65	29.5	5.66	2.228
12	10E	5.08	35	1150	40.3	0.65	29.5	5.66	2.228
13	10W	5.08	25	1150	28.8	0.65	29.5	5.66	2.228
15	11E	5.08	40	1150	46.0	0.65	29.5	5.66	2.228
14	11W	5.08	20	1150	23.0	0.65	29.5	5.66	2.228
17	17E	5.08	39	1150	44.9	0.65	29.5	5.66	2.228
16	17W	5.08	37	1150	42.6	0.65	29.5	5.66	2.228

Table 2. 10.16 cm diameter PICA models and test conditions

Model No.	Run No.	Flat-Face Model Diameter (cm)	Test Time (sec)	Heating Rate (W/cm^2)	Total Heat Load (kJ/cm^2)	Stagnation Pressure (atm)	Enthalpy (MJ/kg)	PICA Thickness (cm)	PICA Thickness (inch)
1	15E	10.16	69	580	40.0	0.45	29.5	6.05	2.380
2	15W	10.16	86	580	49.9	0.45	29.5	6.05	2.380
3A	14E	10.16	20	580	11.6	0.45	29.5	2.24	0.880
3B	13E	10.16	40	580	23.2	0.45	29.5	3.25	1.280
4A	17W	10.16	30	400	12.0	0.20	29.5	2.24	0.880
4B	13W	10.16	20	580	11.6	0.45	29.5	3.25	1.280
5A	17E	10.16	30	400	12.0	0.20	29.5	2.24	0.880
5B	18E	10.16	40	400	16.0	0.20	29.5	3.25	1.280
6A	14W	10.16	20	580	11.6	0.45	29.5	2.24	0.880
6B	18W	10.16	60	400	24.0	0.20	29.5	3.25	1.280
7A	12E	10.16	15	580	8.7	0.45	29.5	2.74	1.080
7B	12W	10.16	15	580	8.7	0.45	29.5	2.74	1.080
8A	11E	10.16	10	580	5.8	0.45	29.5	2.74	1.080
8B	11W	10.16	20	580	11.6	0.45	29.5	2.74	1.080
9A	16E	10.16	15	400	6.0	0.20	29.5	2.74	1.080
9B	16W	10.16	29	400	11.6	0.20	29.5	2.74	1.080

Experimental test data were compared with computed response results to develop and refine an analytical model that would satisfactorily predict both the ablative and thermal performance of PICA heat shields. These comparisons and results for the prediction of Stardust entry performance are given in more detail in following sections.

2.2.1 Test Models

Drawings of the PICA model configurations are shown in Figs. 1 and 2. Typical 2.54 cm and the 5.08 cm diameter models are illustrated in the drawing of Fig. 1 with model and graphite adapter dimensions proportionally scaled depending on the model diameter. The 10.16 cm diameter models are illustrated in Fig. 2. Details of the instrumented 10.16 cm models are shown in Fig. 3. The flat-faced 2.54 cm and 5.08 cm models had a corner radius of 0.239 cm and 0.476 cm, respectively. The 10.16 cm diameter models had a radius of 0.953 cm. All models were fabricated from flight-qualified PICA material from the same processing lot as that used for the Stardust flight heat shield. The average density of the PICA billet used for the models was 0.266 g/cm^3 as determined from small samples taken from multiple locations throughout the billet. The sidewalls of 2.54 and 5.08 cm models were uncoated but nearly all of the 10.16 cm models were coated with a graphite-based slurry (Graphi-Bond®) to minimize the escape of internally-generated pyrolysis gases out the sides.

The 2.54 cm and 5.08 cm models were retained in a graphite adapter using a graphite pin as shown in Fig.1. These graphite adapters were, in turn, attached to a facility model support arm with a stainless steel threaded mounting tube and a boron nitride insulation sleeve. This insulating sleeve was necessary to electrically isolate the model from the grounded support arm and reduce noise on the instrumentation signals.

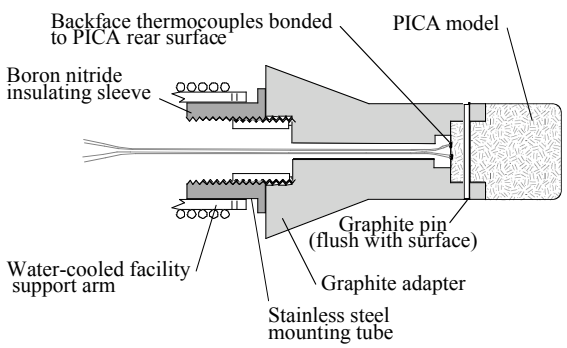

Fig. 1 5.08 cm diameter PICA model

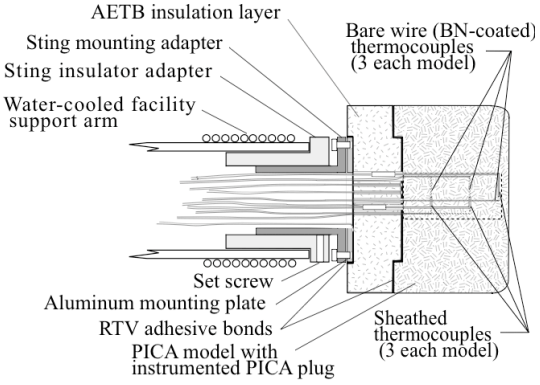

Fig. 2 10.16 cm diameter model

The 10.16 cm diameter models were constructed as shown in Fig. 2 with a 2.54 cm thick layer of Alumina Enhanced Thermal Barrier (AETB) material behind the PICA layer for thermal isolation and approximation of an adiabatic back wall condition. The PICA samples, AETB layers, and aluminum mounting plates were attached to each other with silicone adhesive as indicated in Fig. 2.

2.2.2 Test Model Instrumentation

The high heating rates and resulting high material temperatures used in the arc jet tests resulted in limitations on the type and number of material performance measurement sensors that could be incorporated. Because of the high rate of temperature increase and the high maximum temperatures (>3000˚C) expected in the 2.54 cm and 5.08 cm diameter models, only backface temperature and surface temperature measurements were made on these models. Backface temperatures were obtained using 0.254 mm diameter Type R thermocouples attached to the model rear face with a graphite-based cement (Graphi-Bond®) as illustrated in Fig. 1. Two of these backface thermocouples were attached to each model for redundancy.

The 10.16 cm diameter models were instrumented using multiple thermocouple probes and bare wire thermocouples to measure in-depth, bondline, and backface temperatures. All in-depth sensors were mounted into a 2.54 cm diameter cylindrical PICA core that was subsequently inserted into the larger PICA model.

Only temperature measurements using the sheathed thermocouple probes are reported in this paper; a comparison of the sheathed thermocouple and the bare wire thermocouple measurements will be published separately.

The thermocouple probes were constructed of Type S thermocouple wire of 0.127 mm diameter encased in a 0.508 mm diameter platinum sheath and insulated with MgO powder to prevent electrical shorting to the sheath wall. These sheathed probes were bent at a 90˚ angle 1.27 cm from their tips to provide a configuration that allowed insertion into the test material along a constant depth line assumed to be along an isotherm and normal to the heat flux on the front face of test material. Such a temperature sensing configuration with the sensor wires or sheaths aligned along an isotherm and having a sheath length to diameter ratio of at least 25:1 (as in this case) minimizes measurement error due to conduction losses [8].

Accurate placement of both the sheathed thermocouple probes and the wire thermocouples was assured by insertion into carefully drilled holes at the specified depths measured from the unablated front face of the models. An insulative coating was applied to the wire thermocouples by dipping into a boron nitride slurry and then drying prior to insertion into the models. It was noted, however, that this coating was unevenly removed when the wire was pulled through the models during insertion so that the wire was probably not electrically insulated from the PICA in either the initial virgin or in the charred state.

Thermocouple In-Depth Locations
Distance from plug front face
(All dimensions in cm)

T/C	x	y	z	T/C to be used
1	0.20	-	-	Platinum sheath - Type S
2	-	1.60	-	Platinum sheath - Type S
3	-	-	3.60	Platinum sheath - Type S)
4	0.20	-	-	0.025 D bare wire BN-coated - Type S
5	-	1.60	-	0.025 D bare wire BN-coated - Type S
6	-	-	3.60	0.025 D bare wire BN-coated - Type S
7	In PICA/AETB bondline			Type K
8	In PICA/AETB bondline			Type K
9	In AETB/Al mounting plate bondline			Type K

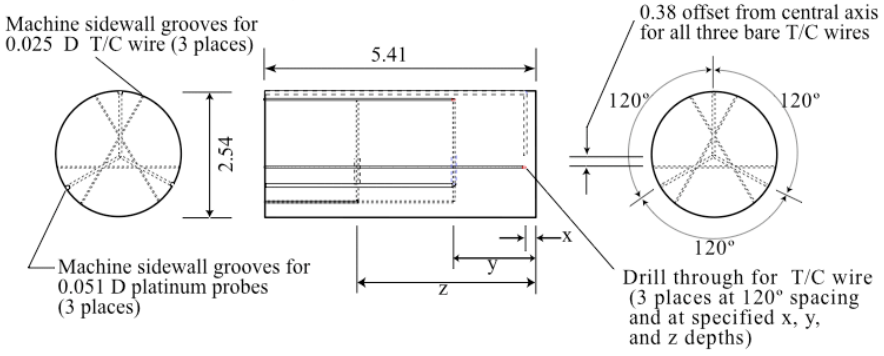

Fig. 3 Typical 10.16 cm diameter model instrumentation details

Bondline temperatures were measured by thermocouples (Type K) mounted within the silicone adhesive bondline between the rear face of PICA models and the AETB layer. Backface temperatures were sensed with thermocouples (Type K) attached to the rear face of this AETB material. Two bondline thermocouples were used on each model for redundancy.

Surface temperature data were obtained using two different single-wavelength optical pyrometers as well as a dual-wavelength (two-color) optical pyrometer. An imaging infrared video pyrometer system also was used to measure temporal temperature distributions on models during tests.

2.1.3 Stream Calibrations

Stream measurements were performed to set the heating rate and pressure conditions for these tests. Stagnation pressure for all arcjet conditions was measured using water-cooled pitot probes. For conditions used with the 2.54 cm and 5.08 cm diameter models, two different hemisphere-cylinder copper heat sink calorimeters were used to measure the cold wall convective heating flux. One calorimeter had a diameter of 3.05 cm and a nose radius of 5.84 cm and the other had a diameter of 3.05 cm and a nose radius of 10.16 cm. Both calorimeters had a corner radius of 0.152 cm. The data from a series of calibration runs with these two calorimeters were used to select two test conditions. One selected condition gave a cold wall, fully catalytic heating rate of 1630 W/cm^2 for tests of the 2.54 cm diameter models. This same condition provided a cold wall, fully catalytic convective heating rate of 1150 W/cm^2 for the 5.08 cm diameter models. The measured stagnation pressure at this test condition for both smaller models was 0.65 atm. The actual measured heating rate values of these non-flat faced calorimeters were corrected using the geometric correlation factors of [9] to provide the assumed heating flux to the flat faced PICA models actually tested. The front surfaces of the copper heat sink mass in these calorimeters were carefully cleaned before each run to assure that a highly catalytic surface for dissociated gas species recombination was present to fulfill the assumption of a fully catalytic wall.

Calibration runs for the 10.16 cm diameter models used 7.62 cm diameter water-cooled hemisphere calorimeters with Gardon-type thin foil heat flux sensors mounted at the stagnation point to define two test conditions. One selected nominal condition for tests of the 10.16 cm diameter PICA models was a cold wall, fully catalytic heating rate of 400 W/cm^2 and a stagnation point pressure of 0.20 atm, and the other was at a heating rate of 580 W/cm^2 and stagnation pressure of 0.45 atm.

2.1.4 Test Environments

The arc jet test conditions and test times are shown in Table 1 for the 2.54 and 5.08 cm diameter models and in Table 2 for the 10.14 cm diameter models. The exposure times for the smaller models varied from 6 sec to 40 sec and resultant total heat loads were from 9.8 kJ/cm^2 to 44.9 kJ/cm^2 (see Table 1). For the 10.16 cm diameter models, the two different arc jet operating conditions provided model exposure times from 10 to 86 sec, and total heat loads from 5.8 kJ/cm^2 to 49.9 kJ/cm^2 on PICA models of varying thickness as shown in Table 2. The arc jet operating conditions for all the tests was at a nominal stream total enthalpy of 29.5 MJ/kg. Radiation heating to the models from the shock layer at all of these conditions was negligible.

2.3 Material Performance Modeling

Modeling of the ablation and thermal performance of the PICA material used the FIAT (Fully Implicit Ablation and Thermal) computer code described in [10]. This code was used in a mode that models in-depth conduction, kinetically-controlled pyrolysis, blowing due to pyrolysis gases, and surface recession as a function of time in a one-dimensional porous ablative material. The PICA properties used with this code were a combination of measured thermophysical properties and polymer pyrolysis kinetics, and adjusted property values based on thermal response data from these tests. The measured specific heat and thermal conductivity of virgin material were taken from [11]. The initial values from [11] for char thermal conductivity and specific heat were iteratively adjusted to give the best fit to thermal response data over the range of test results. The Arrhenius kinetic constants for phenolic pyrolysis from [12] were used. Pyrolysis gas enthalpy values for the ablation products were calculated using an equilibrium thermochemistry program [13]. A PICA virgin and char surface emissivity of 0.9 was assumed that is consistent with the value [2] measured for PICA and that has been used for other carbonaceous ablators. The PICA material ablation model was validated using the arcjet surface recession and thermal response data from these tests as discussed in following sections.

2.4 Data Analysis and Computational Model Comparisons

2.4.1 Ablation Performance

The 2.54 cm and 5.08 cm diameter models were tested at the highest heating rates and stagnation pressures as previously described to measure surface ablation rates at conditions approximating those for a nominal Stardust entry (1200 W/cm^2) and at least a 25% higher heating rate. The surface recession rate is taken as the best measure of ablative performance in this study. The recession rate data for these two smaller models are listed in Table 3, and recession rate data for the 10.16 cm models are given in Table 4. These data are plotted and compared to the steady state surface recession rate calculated by the FIAT code in Figs. 4 and 5. A least squares fit of data at both the 1150 and 1630 W/cm^2

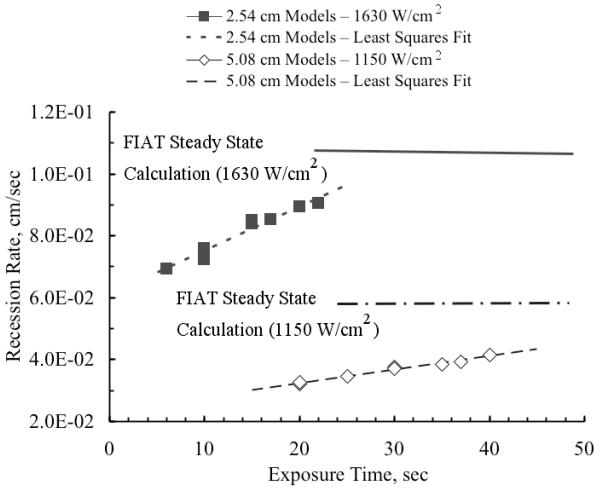

Fig. 4 Surface recession for 2.54 and 5.08 cm models

heating levels show a clear trend of increased recession caused by one or a combination of effects. One effect may be due to the increasing depletion of the phenolic resin at these high heating conditions, thus reducing blowing by pyrolysis gases from the front face and resulting in reduced convective heating blockage. High sidewall heating to the small diameter models under these conditions invalidates the assumption of one-dimensional slab heating inherent in the FIAT calculations. Also, the progressive rounding of the model front face with increasing exposure time and a resulting decrease in the effective nose radius would increase the convective heating. The data in Fig. 4 show that the recession rates for the smaller models approach that predicted by the FIAT code and, at both heating levels, the recession is less than the calculated steady state rate over the range of test times experienced. The data for the surface recession of the 10.16 cm models and comparison with the transient recession rate as calculated by the FIAT code using revised properties are given in Fig. 5. The plot shows that the average measured recession rates for both the 400 W/cm^2 and 580 W/cm^2 levels are higher than that predicted by FIAT code with the predicted steady state rate being 11% low at the 400 W/cm^2 level and 7% low at the 580 W/cm^2 condition. This agreement between measured and predicted recession rates using the FIAT model is satisfactory considering the range of high heating fluxes the model attempts to cover and the test and model parameter uncertainties. The curves for the calculated FIAT response show that, even at the 400-600 W/cm^2 heating range, there is a reasonably long initial period of non-steady ablation of at least 40 seconds until steady state values of surface recession and temperature are

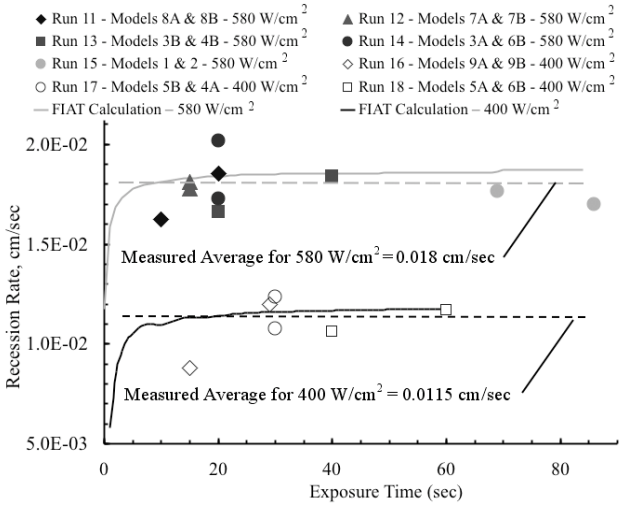

Fig. 5 Surface recession for 10.16 cm models

reached. Recession asymmetries developed on the 2.54 and 5.08 cm models that are thought to be due to misalignment with the peak heating profile in the arc heater stream at the high heating rate conditions, and recession measurements were only made at the center for these models. On the 10.16 cm diameter models, asymmetric recession was not observed and recession measurements were made at the center, 1.0 cm away from the center, and at the edge of the model. The results are shown in Table 4. The front surface roughness on all models tested was greater post-test than on the pre-test machined surfaces; however, the surfaces exhibited no evidence of large scale spallation and visually appeared reasonably smooth and uniform at all conditions.

2.4.2 Thermal Performance

Surface and in-depth temperature measurements from the 10.16 cm diameter models were used to define the thermal response and to derive the analytical response model as previously discussed. The temperature data from a selected number of tests on these models were used to revise the thermophysical properties for use in the FIAT response code. None of the recession data from either the 2.54 cm, 5.08 cm, or 10.16 cm models was used for defining the properties since changes in these properties over ranges of interest have minimal effect on the recession rates. The temperature response data used were those from Models 3B, 4B, 5B, 6A, 6B, 7B, and 9B. These were selected because they were the most complete sets of data, had the best instrumentation signal reliability, and included a representative range of PICA layer thicknesses from 2.24 cm to 3.25 cm and model diameter to thickness ratios from 4.55 to 3.125. The approach used to revise the modeling parameters was to modify only the char conductivity and char specific heat, and re-run the FIAT code for a new set of predictions that was compared with the experimental in-depth temperature profiles for the 8 sets of data from the models selected. This process was then iteratively repeated until it was judged that the revised model predictions were in reasonable agreement with the sets of measured data. The char thermal conductivity and specific heat were chosen as the properties to vary since they are the two with the greatest uncertainty.

Figs. 6 through 11 show representative in-depth and surface temperature data and compare these data with FIAT code predictions using the revised property set that gave the best agreement. In general, the comparison of the agreement is based on maximum temperature reached at a given in-depth location because of an observed temperature rise lag that did not match the predicted monatomic temperature rise of the computer calculations. This failure to predict the observed lag in in-depth and bondline temperatures was found in all data for this and other tests of PICA material, and is discussed more fully later in the paper. The maximum temperature was chosen for this reason as the basis of comparison between measured and predicted results. For each of the temperature plots of Figs. 6 through 10, the legends show in parenthesis the depth of the installed thermocouple probes from the original unablated surface.

The data from model 9B are typical for the lowest heating rate of 400 W/cm^2. Model 9B had a test time of 29 sec and an integrated heat load of 11.6 kJ/cm^2. In-depth thermocouple and pyrometer-measured surface temperature data are presented in Figs. 6a, 6b, and 6c for this model. It is seen that temperatures calculated

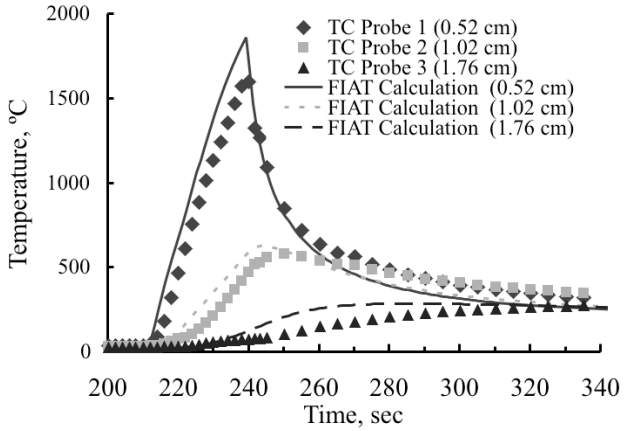

(a) In-depth temperatures

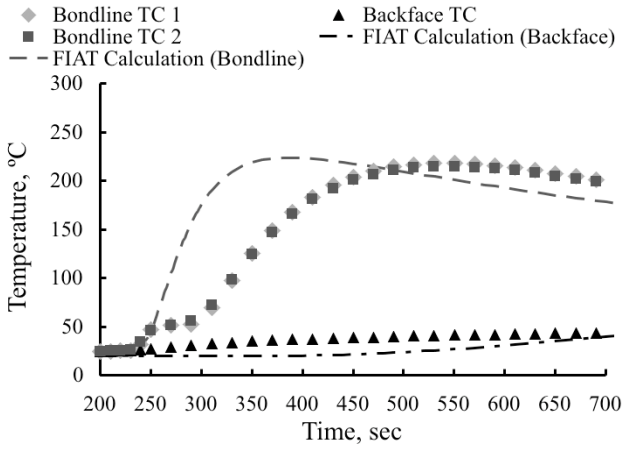

(b) Bondline and backface temperatures

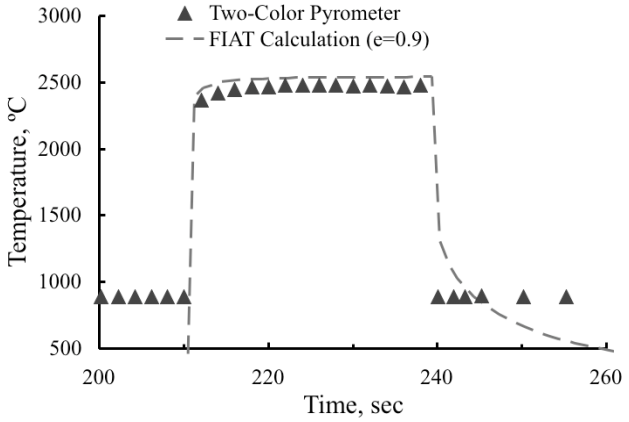

(c) Surface temperature

Fig. 6 Comparison of experimental and calculated thermal response for Model 9B. Heating rate=400 W/cm^2; stagnation pressure=0.20 atm; heating time 29 sec.

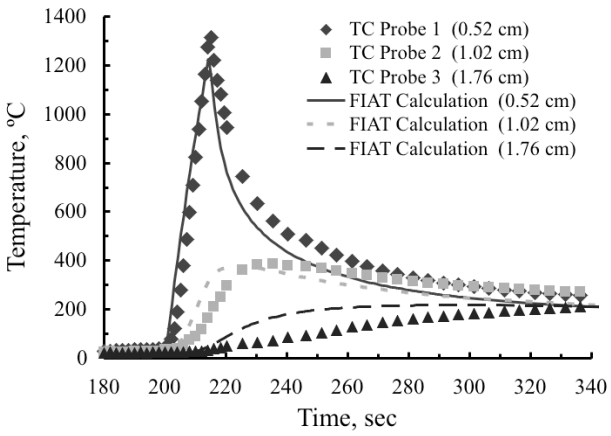

(a) In-depth temperatures

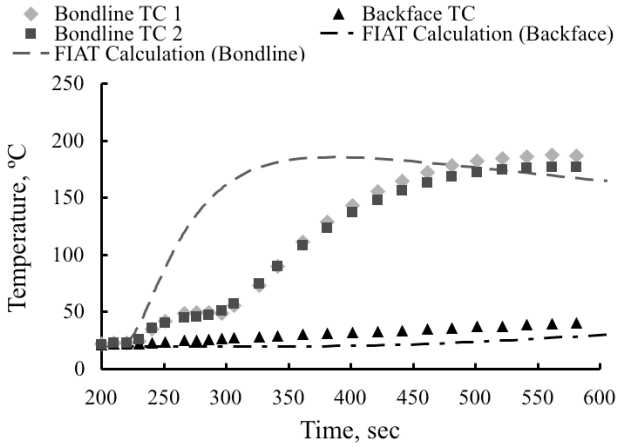

(b) Bondline and backface temperatures

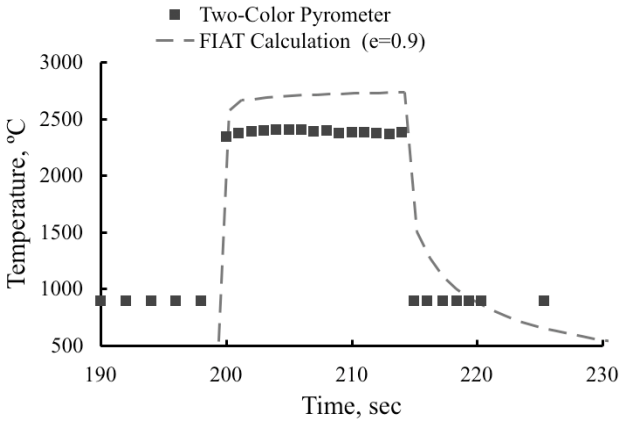

(c) Surface temperature

Fig. 7 Comparison of experimental and calculated thermal response for Model 7B. Heating rate=580 W/cm^2; stagnation pressure=0.45 atm; heating time=15 sec.

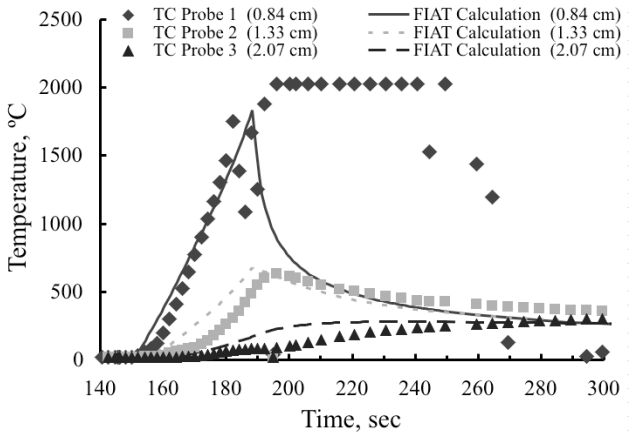

(a) In-depth temperatures

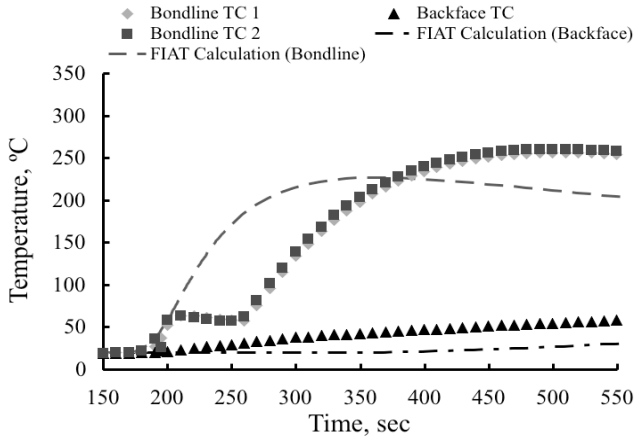

(b) Bondline and backface temperatures

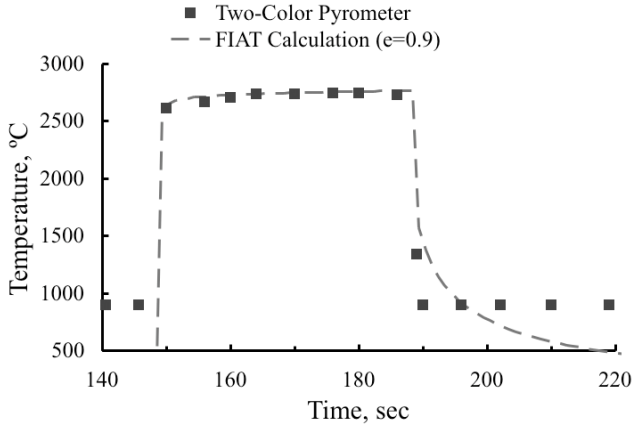

(c) Surface temperature

Fig. 8 Comparison of experimental and calculated thermal response for Model 3B. Heating rate=580 W/cm^2; stagnation pressure=0.45 atm; heating time=40 sec.

with the FIAT code are in reasonably good agreement with the experimental data except for 1) a mismatch in the prediction for the thermocouple closest to the surface (0.52 cm deep), 2) a faster temperature rise than measured for this depth, and 3) a failure to predict the bondline temperature response lag as shown in Fig. 6b.

Figures 7a, 7b, and 7c present a comparison of predicted in-depth, bondline, backface, and surface temperatures from the FIAT code with experimental measurements for Model 7B at a heating rate of 580 W/cm^2. In this case, the code predicts well the response of the thermocouple nearest the surface (0.52 cm deep), the peak in-depth temperatures at 1.016 cm and 1.755 cm depth, and the maximum bondline and backface temperatures. The measured surface temperature is about 300˚C lower than the calculated level but is unaccountably lower than other pyrometer-measured temperatures at this same heating condition. Again, the calculated response does not accurately simulate the lag in temperature rise at the 1.02 cm and 1.76 cm deep locations or at the bondline.

The data from the test of Model 3B show similar results in Figs. 8a, 8b, and 8c. For this model, Fig. 8a shows that the thermocouple probe melted at about the temperature expected for platinum (1769˚C). The FIAT calculation is seen to predict well the maximum temperatures measured at 1.33 and 2.07 cm depths, and the maximum of the two bondline temperatures, but the calculated response did not match the lag in the measured temperature rise seen in Figs. 8a and 8b. The calculated and experimental surface temperatures are seen to be in excellent agreement in this case for the entire test time (Fig. 8c). Another example presented for results at a heating level of 580 W/cm^2 is given in Fig. 9a, 9b, and 9c for Model 6A. This is the thinnest 10.16 cm diameter model tested with a pre-test thickness of 2.24 cm. The thermocouple probe closest to the surface (0.52 cm deep) melted at a temperature consistent with the melting point for platinum (Fig. 9a) as would be expected. The other response of the other in-depth thermocouple (1.43 cm deep) is matched by the computer prediction for maximum temperature (Fig. 9b). The calculated and measured surface temperatures are seen to agree well (Fig. 9c).

Fig. 10 shows results for Model 2 tested at a heating rate of 580 W/cm^2 for the longest test times and highest integrated heat load of all the 10.16 cm models. This model was heated for 86 seconds with a total heat load of 49.9 kJ/cm^2. Both of these two tests exceeded the total heat load value (36 kJ/cm^2) expected for the Stardust SRC entry with the nominal entry trajectory

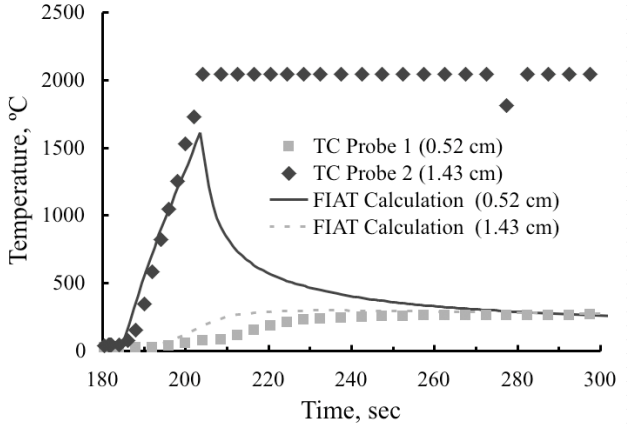

(a) In-depth temperatures

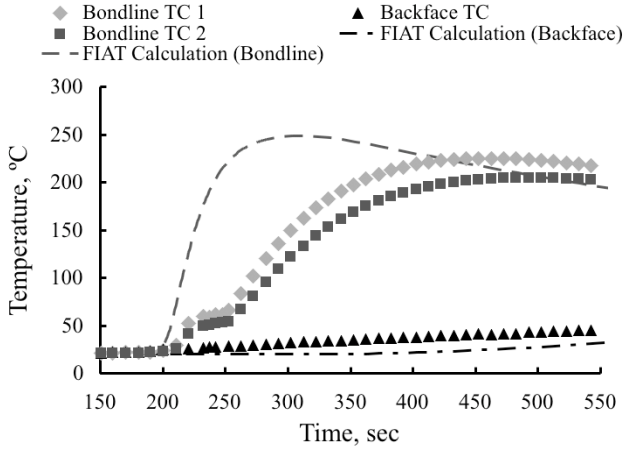

(b) Bondline and backface temperatures

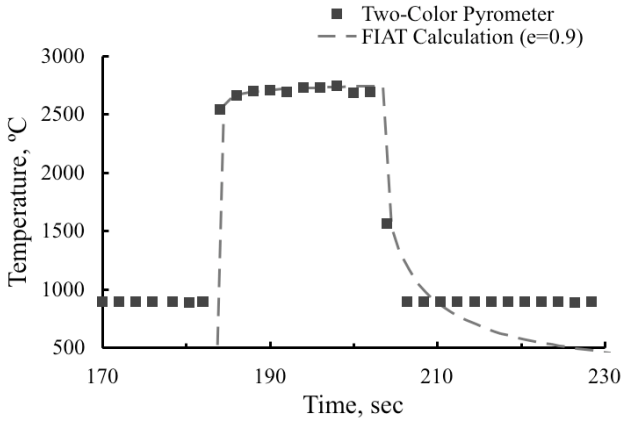

(c) Surface temperature

Fig. 9 Comparison of experimental and calculated thermal response for Model 6A. Heating rate=580 W/cm^2; stagnation pressure=0.45 atm; heating time=20 sec.

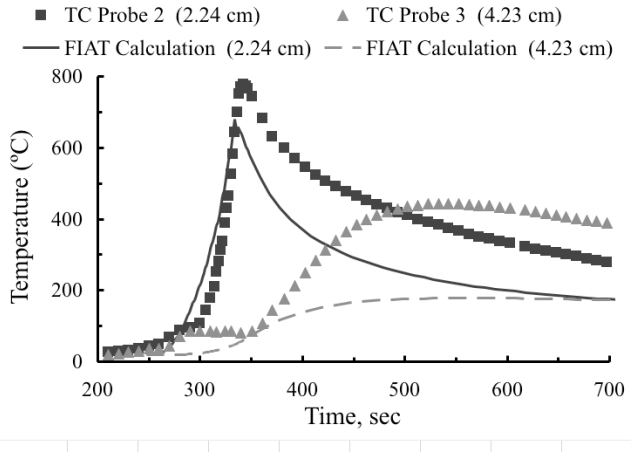

(a) In-depth temperatures

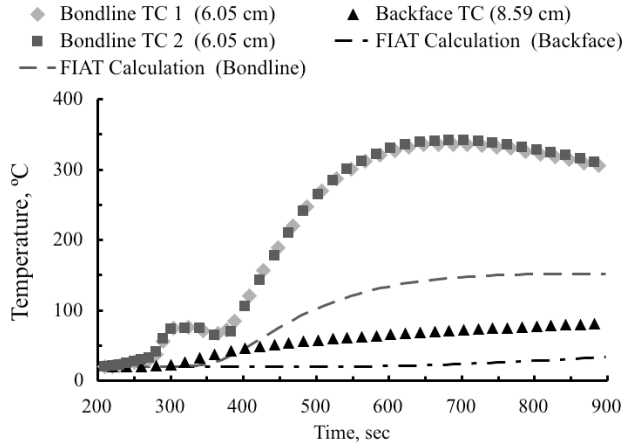

(b) Bondline and backface temperatures

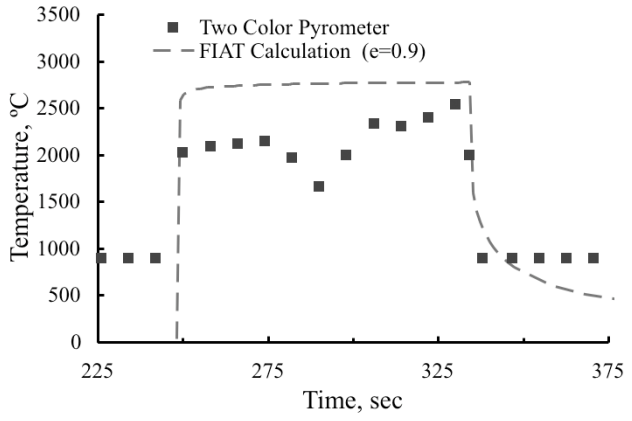

(c) Surface temperature

Fig. 10 Comparison of experimental and calculated thermal response for Model 2. Heating rate=580 W/cm^2; stagnation pressure=0.45 atm; heating time=86 sec.

but were somewhat less than the expected heat load of 55 kJ/cm^2 for an overshoot trajectory entry. This was one of the two thickest models tested with 6.04 cm of PICA backed by the 2.54 cm thick AETB layer. The thermocouple probes closest to the surface (0.89 cm deep) indicated failure from melting within the first 20 seconds of exposure with a response very similar to that shown for Model 3B and Model 6A (see Figs. 8a and 10a) and not shown here.

In Figs. 10a, 10b, and 10c, it is seen that the computer model results badly under-predict the in-depth, bondline, and backface measured temperatures in contrast to the much better agreement on thinner PICA models. The best explanation for this FIAT underprediction is that the assumption of one-dimensional ablation and heat conduction inherent in the FIAT model is not valid on these thick models with a large side wall area exposed to high heating levels. This conclusion is also supported by temperature rise differences between the computer predictions and the measured values. The more rapid onset of the measured in-depth temperature rise seen in Figs. 10a, and 10b is consistent with heat being conducted inward from sidewall heating. A post-test cross-section photo (Fig. 11) of one of these models after being cut into two halves clearly shows that considerable degradation had progressed from the model sides toward the center, thus invalidating the assumption of one-dimensional heat transfer assumed in FIAT calculations.

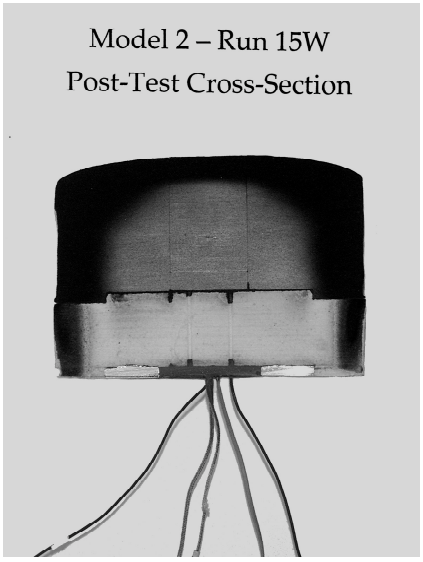

Fig. 11 Post-test photo of Model 2 cross-section that shows internal ablation resulting from sidewall heating

The measured in-depth temperature data characterized by an expected increase with time followed by a leveling off at temperatures between 0ºC to 100ºC to a constant or, in some cases, a decreasing temperature value (cf., Figs. 6b, 7b, 8b, 9b, 10a, 9b, 11b) has been observed in other heating tests of PICA and similar phenolic impregnated materials. For example, this same feature is evident in temperature data from arcjet tests during PICA development [14]. Similar features are seen in data from other heating tests of materials with phenolic resin impregnation dating back to at least 1968 but apparently have not been documented. An unidentified endothermic process within the PICA material can explain this behavior. Phase transition processes are known to cause similar effects on transient temperature data in other materials. It is clear that the FIAT code with the material properties and ablation chemical kinetics used for this study did not capture this behavior. The resolution of this modeling inconsistency is the subject of a separate investigation.

3. APPLICATION TO STARDUST FLIGHT HEAT SHIELD DESIGN

An objective of this investigation was to verify the Stardust SRC forebody heat shield design for Earth re-entry. The major design criterion for this vehicle heat shield was a maximum allowable bondline temperature of 250˚C. The revised PICA properties derived from iterative adjustment to provide a best fit to data shown herein was used with the FIAT computer code to recalculate the surface recession, maximum temperatures, and design margins. Fig. 12 presents the results of this newer calculation and a comparison to the original design with the calculated bondline temperature as a function of spacecraft entry time plotted for both the baseline design trajectory heating rate (1200 W/cm^2) and for a 25% increase in heating rate (1500 W/cm^2). The result from the original calculation using the baseline Stardust properties also is shown. It is seen that the calculated maximum bondline temperatures for the cases of nominal design heating and of a 25% added margin are all well below the design maximum allowable temperature of 250˚C. The recalculated maximum temperature of about 116˚C is also less than that from the earlier calculation with baseline properties of 190˚C. These results provide added confidence in the performance of PICA material for the Stardust heat shield design.

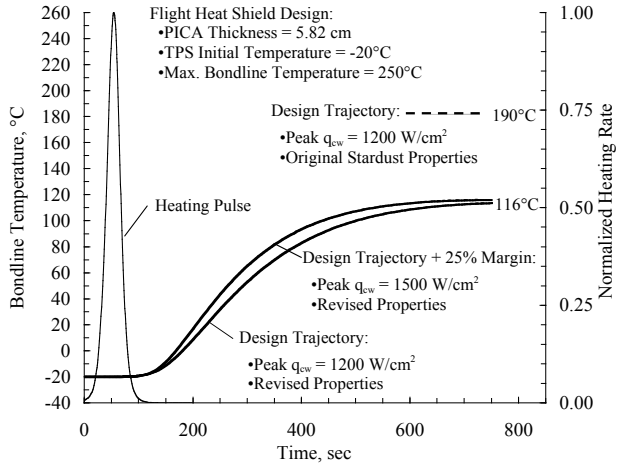

Figure 12 Comparison of Calculated bondline temperatures for Stardust heat shield design using baseline and revised model properties

4. Concluding Remarks

Extensive arcjet tests at conditions simulating the design Earth entry heating conditions for the Stardust Sample Return Capsule were conducted as part of this investigation to evaluate the heat shield design. The resulting data on ablative surface recession and internal temperature response were used to iteratively modify thermophysical properties for PICA material used in the FIAT computer code to satisfactorily predict the experiment response using surface recession rate and maximum internal temperatures as criteria. An apparent endothermic process at low temperatures during PICA ablation resulted in a delayed internal temperature rise that was not captured by computer code results using either the baseline or the revised properties. A separate study is underway to investigate this previously undocumented process. The predictive results using the FIAT code, however, were in reasonable agreement with measured surface recession and maximum internal temperature data so that the use of this code with the revised property set can predict with good confidence the performance of the actual Stardust heat shield design. It was concluded that the results of this study have validated the original Stardust PICA forebody heat shield design, and provided evidence for lower than previously predicted maximum temperatures at the adhesive bondline attaching the shield to the spacecraft structure. These results increase confidence in the heat shield design for the Stardust Sample Return Capsule.

Acknowledgments

This work was supported by NASA Ames Research Center under Contract NAS2-99092 with Eloret Corporation. The assistance of Bill Willcockson of the Lockheed Martin Company in providing data and material is gratefully acknowledged. The authors would like to thank James Arnold and Ethiraj Venkatapathy of NASA Ames for continued support and their valuable comments and suggestions.

References

1. Vellinga, J. , et al, "Environmental Design Considerations for Stardust," Report 97ES-197, Lockheed Martin Company, Januaary 1997.
2. Tran, H., Johnson, C.E., Rasky, D.J., Hui, F.C., Hsu, M.-T., Chen, T., Chen, Y.-K., Paragas, D., and Kobayashi, L., "Phenolic Impregnated Carbon Ablators (PICA) as Thermal Protection Systems for Discovery Missions," NASA TM-110440, April 1997.
3. Tran H., Johnson, C.,Hsu, M-T., Smith, M., Dill, H., Chen-Jonsonn, A., "Qualification of the Forebody Heatshield of the Stardust's Sample Return Capsule," Paper 97-2482, 32nd AIAA Thermophysics Conference, Atlanta, Georgia, June 23-25, 1997.
4. Covington, M.A., Goldstein, H.E., Balboni, J.A., Terrazas-Salinas, I., Chen, Y.-K., Olejniczak, J., Martinez, E.R., Hienemann, J.M., "Analysis and Modeling of the Performance of a Low Density Carbon Phenolic Material for Atmospheric Entry Thermal Protection," NASA TM (to be published).
5. Winovich, W., and Carlson, W., "The 60 MW Interaction Heating Facility," 25th International Instrumentation Symposium, Anaheim, California, May 1979.
6. Olynick, D., Chen, Y.K., and Tauber, M., "Forebody TPS sizing with Radiation and Ablation for the Stardust Sample Return Capsule," Paper 97-2474, AIAA 32nd Thermophysics Conference, Atlanta, GA, June 23-25, 1997.
7. Zoby, E.V., "Empirical Stagnation-Point Heat Transfer Relation in Several Gas Mixtures at High Enthalpy Levels," NASA TN D-4799, June 1968.
8. Anon., *Standard Practice for Internal Temperature Measurements in Low-Conductivity Materials*, ASTM Standard E-377, December 1996.
9. Zoby, E.V. and Sullivan, E.M.,"Effects of Corner Radius on Stagnation-Point Velocity Gradients on Blunt Axisymmetric Bodies," NASA TN X-1067, March 1965.
10. Chen, Y.-K., and Milos, F.S., "Ablation and Thermal Response Program for Spacecraft Heatshield Analysis," Paper 98-0273, AIAA Aerospace Sciences Meeting & Exhibit, 36th, Reno, NV, Jan. 12-15, 1998.
11. "Final Report on Thermal Properties of Lightweight Charring Ablators," FMI EMTL Final Report No. 1648, Fiber Materials, Inc., July 1994.
12. Goldstein, H.E., et al, *J. Macromolecular Science-Chemistry*, A(34), PP.649-673, July 1969.
13. Anon., "User's Manual, Aerotherm Chemical Equilibrium Computer Program, (ACE81)," Acurex Report UM-81-11/ATD, Acurex Corporation, Aerotherm Division, Mt. View, California, August 1981.
14. "An Assessment of the Influence of Material Variables on the Ablation Response of PICA Type Materials," FMI Report FMI-Pm0-96-036, Fiber Materials, Inc. February 1996.